A second category of nonvalid prompt coincidences are *scatter coincidences.* These occur when one (or both) of the photons from an annihilation event outside the sensitive volume for true coincidence events undergoes scattering and is detected in a detector other than the one that would be appropriate for a true coincidence event. The scattering event shown in (figure 6) occurs within the patient, but it also can occur within components of the scanner. Because the two annihilation photons were emitted simultaneously, they reach the detectors virtually simultaneously, apart from small time-of-flight differences.

As is the case for the random-to-true coincidence ratio, the ratio of scatter-to-true coincidence counting rates depends in a complicated way on the source distribution and detector geometry. Placement of lead shielding on either side of the detector ring, or of thin tungsten septa between detector rings in a multi-ring PET system, reduces the likelihood of accepting scattered photons. Scatter coincidences provide incorrect localization of the positron annihilation event. The degree of position error depends on the scattering angle and location of the scatter event.

5. PET Detector and Scanner Designs

Detection efficiency is an important parameter in PET scanner sensitivity and performance. Sodium iodide detectors, which are the “workhorse” for many nuclear medicine applications, also have been used for PET scanners. However because of the relatively high energy of the 511-keV annihilation photons, sodium iodide generally is not the detector material of choice for PET imaging. For these reasons, most PET scanners use denser higher-Z scintillation detectors arranged in rings or banks of discrete elements around the scanned object. These systems not only provide high detection efficiency but they allow the simultaneous collection of data for all projection angles with a completely stationary set of detectors.

5.1. Block Detectors

Early PET systems used individual detector units consisting of a piece of scintillator coupled to a photomultiplier tube (PMT). The individual detectors were arranged in a ring or in multiple rings around the subject. The

response profile at mid-plane of a pair of coincidence detectors is a triangle with FWHM equal to one half the width of the detector. Thus to improve the intrinsic resolution of a PET scanner, the detectors must be made smaller. However, the cost increases rapidly if each detector element requires its own PMT. The block detector allows small detector elements to be used (improving spatial resolution) while reducing the number of PMTs required to read them out (controlling cost).

Figure (7) shows a typical block detector. A large piece of scintillator (most commonly BGO, LSO, or LYSO), is segmented into an array of many elements by making partial cuts through the crystal with a fine saw. The cuts between the elements are filled with a reflective material that serves to reduce and control optical cross-talk between scintillator elements.

The array of crystals is read out by four individual PMTs. The depth of the saw cuts is determined empirically to control the light distribution to the four PMTs in a fairly linear fashion. To determine the segment of the crystal in which an annihilation photon is detected, the signals from a four-PMT array are combined as follows:

$$X = \frac{(PMT_A + PMT_B) - (PMT_C + PMT_D)}{PMT_A + PMT_B + PMT_C + PMT_D}$$

$$Y = \frac{(PMT_A + PMT_C) - (PMT_B + PMT_D)}{PMT_A + PMT_B + PMT_C + PMT_D} \quad (3)$$

where PMTA, PMTB, and so forth are the signals from different PMTs. It will be recognized that these are essentially identical for position localization for an Anger camera, except that only four PMTs are used here. The X and Y signals then are used to determine the sub element of the array in which the annihilation photon was detected.

Figure (8) shows the image obtained from uniform irradiation of a block detector. The image is not uniform. Rather, the calculated locations for recorded events are clustered in small localized areas corresponding to the individual detector elements. There is a small amount of overlap, but the individual elements are clearly resolved.

Although the array pattern is nonlinear, the separation is sufficiently clear to allow each (x,y) location in the image to be assigned to a specific detector element in the array, for example, by using a look-up table. The major advantage of the block detector is that it enables many detector elements (e.g., 8 × 8 = 64) to be decoded using only four PMTs. This dramatically lowers the cost per detector element while providing high spatial resolution. Typical block detectors are made from 20- to 30-mm- thick BGO, LSO, or LYSO scintillator crystals, with 4- to 6-mm-wide sub-elements.

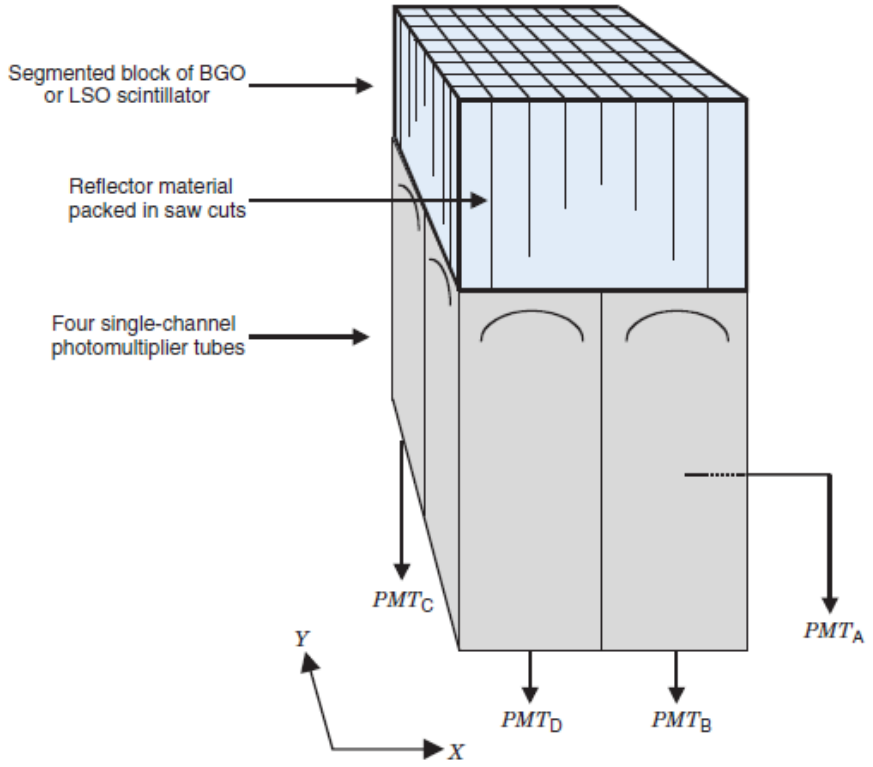

Figure (7): Block detector commonly used in clinical PET scanners.

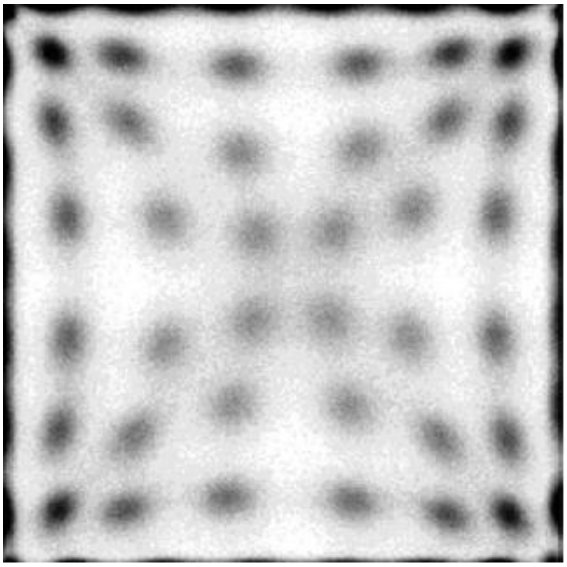

Figure (8): Flood-field image obtained by uniformly irradiating a block detector with 511-keV annihilation photons. Individual block detector elements appear as distinct “blobs” in the image, allowing separation of events recorded within individual detector elements.

5.2. Whole-Body PET Systems

Figure (9) illustrates several different whole-body PET scanner designs that have been developed, some using block detectors comprising discrete scintillator elements as introduced previously (A, B, C) and others that use continuous large-area gamma camera detectors (D, E, F). Systems that use a stationary ring or polygonal array of detectors (A, C, E, and F), with the detectors operating in multi coincidence mode, can acquire data for all projection angles simultaneously and these designs have been the basis for most commercial systems. Others (B, D) use only a few opposing banks of detectors, which must be rotated to get full tomographic information. Most PET systems use a ring diameter of 80 to 90 cm. After inserting scatter shielding and a shroud to cover the detectors and other components, the clear bore of the scanner typically is 55 to 60 cm, which is sufficient to comfortably accommodate most patients. The FOV in the axial direction is determined by the axial extent of the detectors and typically is in the range of 15 to 40 cm.

Figure (10) shows schematically the design of a representative whole-body PET scanner based on block detectors. This scanner employs 336 BGO

block detectors, arranged in three rings of 112 blocks per ring.4 Each block is cut into a 6 × 6 array of elements, with element sizes of 4 mm (trans axial) × 8.1 mm (axial) × 30 mm (thickness). The inside diameter of the detector ring is 92.7 cm and the clear bore of the scanner is 59 cm. The 18 crystals (three rings of three blocks) in the axial direction cover an axial FOV of 15.2 cm. The gantry can be tilted ± 20 degrees from the vertical, which can be useful for aligning the scan planes with the optimal viewing angle for an organ of interest. The system contains a set of tungsten inter plane septa of 1-mm thickness and 12-cm length between the crystal rings. The septa can be extended or retracted to provide varying levels of scatter rejection.

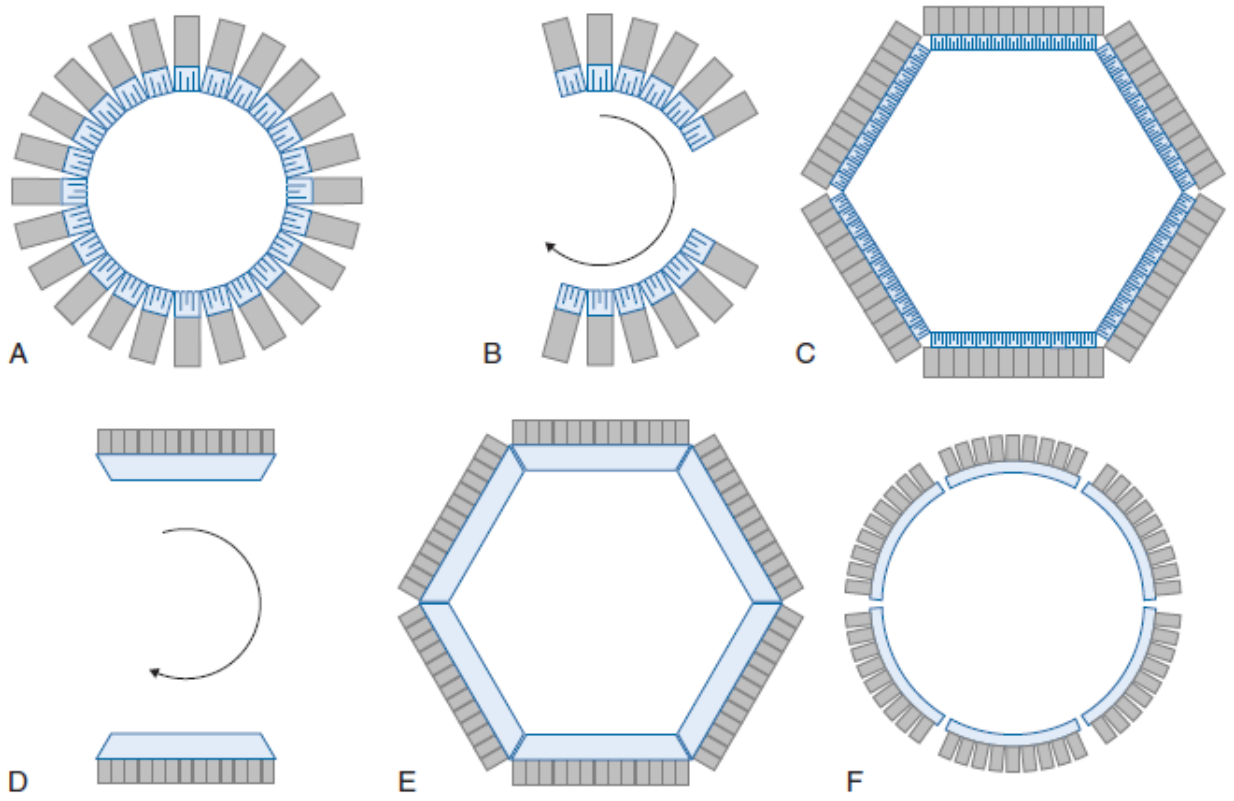

Figure (9): PET scanner geometries based on discrete scintillator elements (top row) or continuous scintillator plates (bottom row). A, Full ring of modular block detectors. B, Partial ring of modular block detectors. C, Hexagonal array of quadrant-sharing panel detectors. D, Dual-headed gamma camera with coincidence circuitry. E, Hexagonal array of gamma camera detectors. F, Continuous detectors using curved plates of NaI(Tl). A complete set of profiles can be acquired without motion with systems shown in A. C, E, and F, whereas detector motion is required with systems shown in B and D.

They also provide shielding from potential high concentrations of activity outside the scanning volume of interest, which helps control the random and scatter coincidence rates. The scanner also incorporates a rod source made from 68Ge (T1/2 = 273 days) to perform transmission scans for attenuation corrections. The source is permanently mounted in the system and is retracted into a lead shield when not in use.

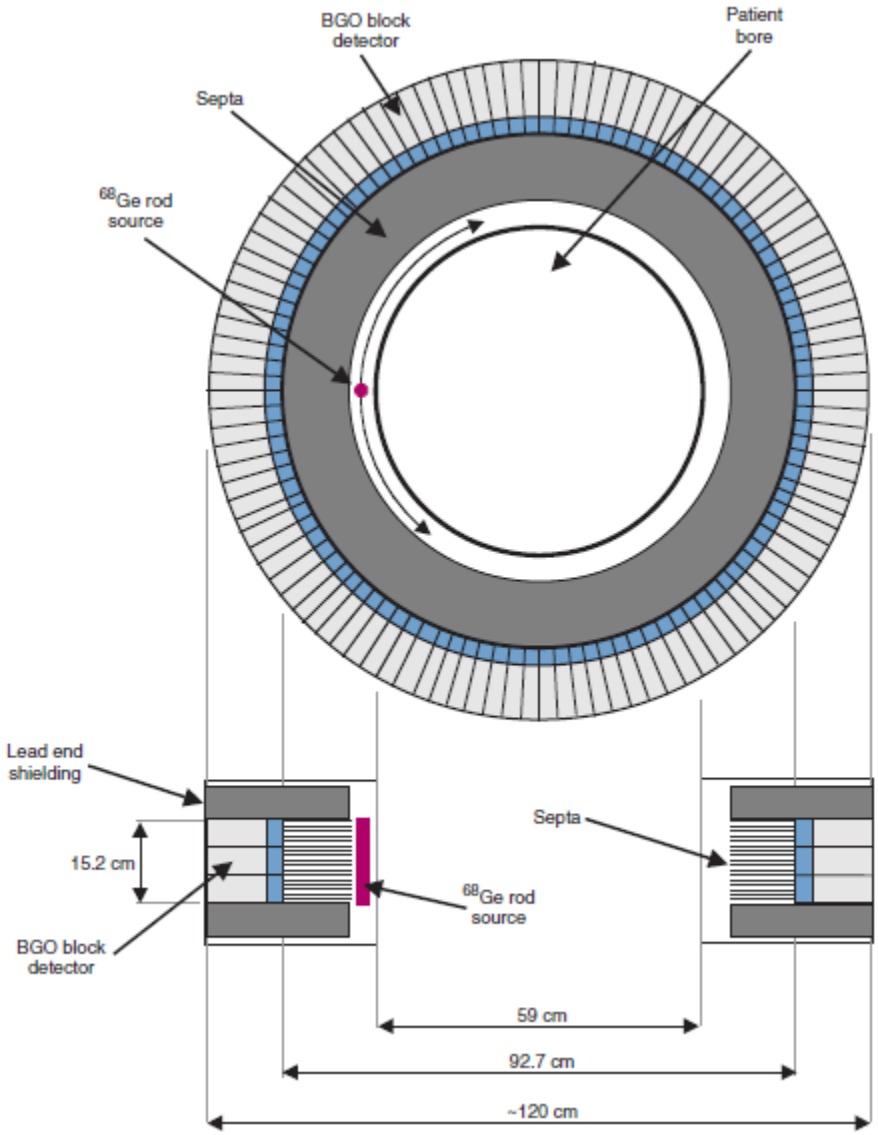

Figure (10): Drawings showing transaxial (top) and axial (bottom) cross-sections through a representative whole body PET scanner.

The intrinsic spatial resolution of the detectors is approximately 3 mm, whereas the system resolution is approximately 4.5 mm near the center of

the FOV and approximately 6.2 mm near the periphery of the scanner bore, the difference being due primarily to DOI effects.

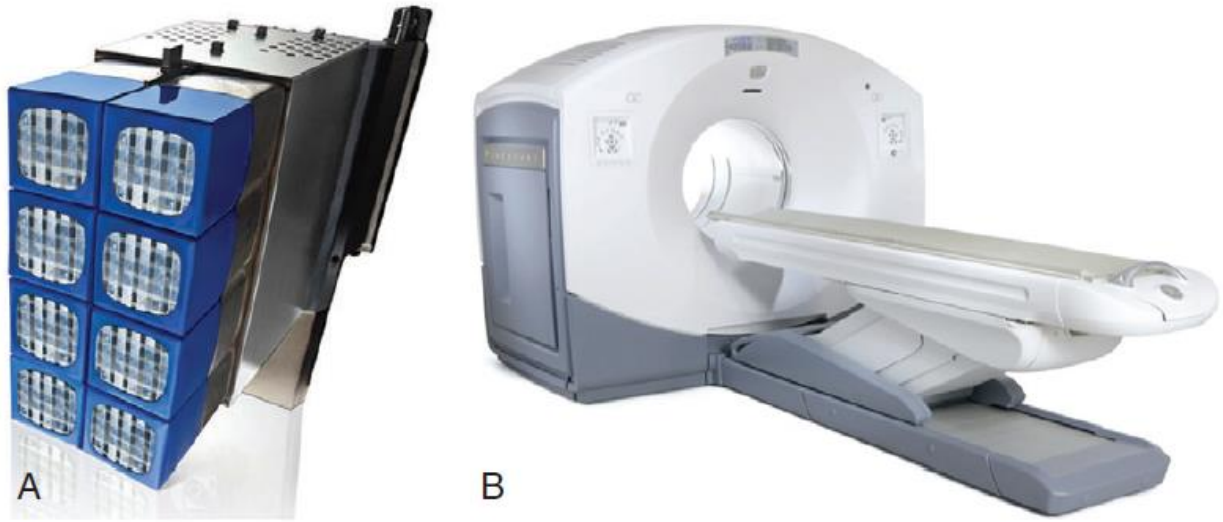

Figure (11):A, Modular cassette from a PET scanner containing eight block detectors. These cassettes are mounted on the PET scanner gantry to form complete rings of detector blocks that surround the patient. B, Clinical PET scanner based on rings of these block detectors.

Gamma camera technology similar to that used for conventional planar imaging and SPECT, also has been employed for PET imaging. In one approach, coincidence timing circuitry has been installed between the heads of dual headed scanners and the collimators removed for PET imaging. The spatial localization provided by the detector heads allows many coincidence lines to be acquired simultaneously. The basic concept is illustrated in Figure (9-D). These systems can still be used for planar or SPECT imaging, by replacing the collimators.

The performance of standard gamma cameras for PET suffers from a number of limitations. Chief among these is the relatively low detection efficiency of the camera detectors for 511-keV annihilation photons. As well, although removing the collimator allows simultaneous data acquisition for many projection angles, the resulting high counting rates can lead to significant dead time losses and pile-up effects. An event detected anywhere in the detector can affect all other events detected at the same time. By contrast, dedicated PET systems use blocks of detectors that

operate essentially independently from each other. Random and scatter coincidence rates, both of which increase with the geometric efficiency for detecting events outside the true coincidence volume, also tend to be high when the collimators are removed from the camera heads. Some manufacturers addressed these limitations by incorporating thicker NaI(Tl) crystals (up to 2.5 cm) into systems intended for PET usage, and by employing more sophisticated circuitry in their gamma cameras to minimize dead time and suppress pile-up effects. Other manufacturers have developed gamma camera detectors specifically for use in PET. One such scanner used six curved gamma camera detector plates, arranged in a ring around the object (Figure 9-F). At the present time, PET scanners based on continuous gamma camera detectors are not widely used. PET systems have been integrated with x-ray computed tomography (CT) technology to create combined PET/CT scanners in a single gantry. Almost all PET scanners sold today are combined with CT.

6. The Gamma Camera

6.1. System Components

Figure (14) illustrates the basic principles of image formation with the gamma camera. The major components are a collimator, a large-area NaI(Tl) scintillation crystal, a light guide, and an array of PM tubes. Two features that differ from the conventional NaI(Tl) counting detectors are crucial to image formation.

The first is that an imaging collimator is used to define the direction of the detected γ rays. The collimator most commonly consists of a lead plate containing a large number of holes. By controlling which γ rays are accepted, the collimator forms a projected image of the γ-ray distribution on the surface of the NaI(Tl) crystal. The second is that the NaI(Tl) crystal is viewed by an array of PM tubes, rather than a single PM tube. Signals from the PM tubes are fed to electronic or digital position logic circuits, which determine the X-Y location of each scintillation event, as it occurs, by using the weighted average of the PM tube signals.